S. Bernardie · N. Desramaut · J.-P. Malet · M. Gourlay · G. Grandjean

Prediction of changes in landslide rates induced by rainfall

Abstract This work focuses on the development of a combined statistical-mechanical approach to predict changes in landslide displacement rates from observed changes in rainfall amounts. The forecasting tool FLAME (Forecasting Landslides Accelerations induced by Meteorological Events) associates (1) a statistical impulse response (IR) model to simulate the changes in landslide rates by computing a transfer function between the input signal (e.g. rainfall) and the output signal (e.g. displacement) and (2) a simple 1D mechanical (MA) model (e.g. viscoplastic rheology) to take into account changes in pore water pressure. The models have been applied to forecast the displacement rates at the Super-Sauze landslide (South East France). The performance of different combinations of models (IR model alone, MA model alone and a combination of the IR and MA models) is evaluated against observed changes in pore water pressures and displacement rates at the study site. Results indicate that the three models are able to reproduce the displacement pattern in the general kinematic regime (succession of acceleration and deceleration phases); conversely, extreme kinematic regimes such as fluidization of part of the landslide mass are not being reproduced. The approach constitutes however a robust tool to predict changes in displacement rates from rainfall or groundwater time series.

Keywords Landslide · Displacement pattern · Prediction · Monitoring · Early warning

Introduction

Forecasting the displacement pattern of continuously active landslides is a challenge for scientists and risk managers. Changes in displacement rates over time are mostly controlled by hydro-meteorological triggers (e.g. rainfalls, rapid snowmelt) and the consequent increase of pore water pressure and by changes in geomorphology (e.g. changes in landslide geometry and stress conditions, changes in material rheology).

Prediction of rainfall-induced landslides is complex since a lot of variables may have a large influence on this phenomenon (Michiue 1985), namely mechanical and hydraulic slope properties, slope morphology, presence of vegetation, and the rainfall features (intensity, duration). Most of the landslides' monitoring systems consist of measurements of rain, pore water pressure and displacements.

The most used and reliable approach to forecast the time of failure at a single slope scale makes use of displacement (and its derivative, velocity) observations. This is based on the fact that, viewed over a long period of time, measured slope displacements may take the form of a standard creep curve, wherein accelerating slope displacements are taken as a warning of imminent failure (Fukuzono 1990; Kawamura 1985; Voight 1988; Zvelebill and Moser 2001; Petley et al. 2005; Eberhardt 2008; Mufundirwa et al. 2010). However, because the fundamental physics controlling the nature and shape of the creep curves has not yet been cleared up, a degree of uncertainty exists in such estimates (Hutchinson 2001).

Other approaches consider the use of rainfall thresholds to analyse the relationship between the triggering precipitation and the movement. The threshold may correspond to a critical value above which the probability of landslide occurrence is higher. Intensity-duration (I-D) thresholds are the most common type of empirical threshold (Caine 1980; Cancelli and Nova 1985; Wieczorek 1987; Larsen and Simon 1993). For homogeneous slope conditions, the assumption is that landslides may occur once a precipitation threshold is reached. In most cases, the threshold equations are defined without any rigorous mathematical statistical or physical criterion, when visualizing the logarithmic plot of the intensity-duration of rainfall events (Guzzetti et al. 2007). I-A-D (intensity-antecedent rain-duration) models are based on a power law function defining a lower bound to global observations of landslide-triggering storms. This function has been widely used for estimating thresholds at all geographic scales (Guzzetti et al. 2008).

Other threshold models are based on dynamic temporal analyses of the rainfall pattern. The FLaIR model (Sirangelo and Versace 1992) estimates slope susceptibility through the identification of a mobility function Y() obtained by the convolution between rainfall Intensity R() and a transfer function psi(), considered as an indicator of slope stability. The model connects then this function to the probability of a new landslide movement. In the FLaIR model, the shape of the transfer function depends on the geotechnical characteristics of the landslide (Sirangelo et al. 2003). It allows analysing the influence of short-term and long-term rainfall components (Capparelli and Tiranti 2010) and has been applied to several documented case studies (Capparelli and Versace 2010; Versace and Capparelli 2008; Greco et al. 2013).

However, the aforementioned methods do not explicitly consider observed and measured landslide quantities, as they are based on a binary classification (e.g. occurrence or not of a landslide). Analysing the temporal component of a landslide constitutes thus a major improvement in the development of forecasting methods, as suspended and dormant landslides can be reactivated in periods of heavy rainfall, while active landslides may show phases of acceleration and deceleration (Flageollet 1996; Corominas 2000).

As a consequence, multi-observation prediction strategies (e.g. forecasting the time to failure with different observations and models) are being developed (Intrieri 2012). Such models aim at describing the relationships among time series of measured quantities such as displacement rates (considered as the output time series) and, for instance, rainfall, pore water pressure and soil moisture (considered as the input time series).

Several models exist to analyse these relationships such as the finite impulse response (FIR) model, the Box-Jenkis (BJ) model, the output-error (OE) model, the autoregressive moving average with exogenous inputs (ARMAX) model, and the autoregressive with exogenous inputs (ARX) model. Artificial neural network (ANNs) techniques (Mayoraz et al. 1996) have also been used to

extract time scales and functionals among multi-parameter time series in order to predict, for instance, pore water pressure as a function of the rainfall, velocity as a function of pore water pressure or velocity as a direct function of rain. Such type of models has for instance, been applied to the Chénaula, Sallèdes and La Frasse landslides with relative good accuracy (Mayoraz and Vulliet 2002).

In addition, simple or complex fully coupled hydro-mechanical models can be introduced in the forecasting framework (van Asch et al. 2007a). Application of these models necessitates to characterize the physical mechanism initiating a landslide (through slope stability analyses; Maugeri et al. 2006) and to use stress-strain models to compute landslide dynamics (Corominas et al. 2005; van Asch et al. 2007b; Pouya et al. 2007). For instance, Angeli et al. (1998) proposed a simple reservoir conceptual model to model the water flow discharge and the groundwater level within a slope and then considered a mechanical viscoplastic model to predict the velocity based on equilibrium equations. In the approach developed by Calvello et al. (2007), the hydrological component is computed using a finite element approach, whereas the displacement rate is obtained from an empirical relationship between the safety factor of the slope and the velocity. The approach developed by Herrera et al. (2009) considers a simple consolidation equation to relate effective rainfall intensity and dissipation of the excess pore pressure; the landslide kinematic is then computed by considering a viscoplastic rheology.

The objective of this work is thus to develop a combined statistical-mechanical model to investigate multi-parametric times series of landslide displacements, pore water pressure and rainfall in order to define possible causal inferences among the triggers and the responses of the slope and to predict the slope kinematics. Three combinations of models are tested. The first model uses a statistical impulse response (IR) function (e.g. TEMPO; Pinault and Schomburgk 2006), which allows us to predict the changes in the landslide rate by computing the transfer function between
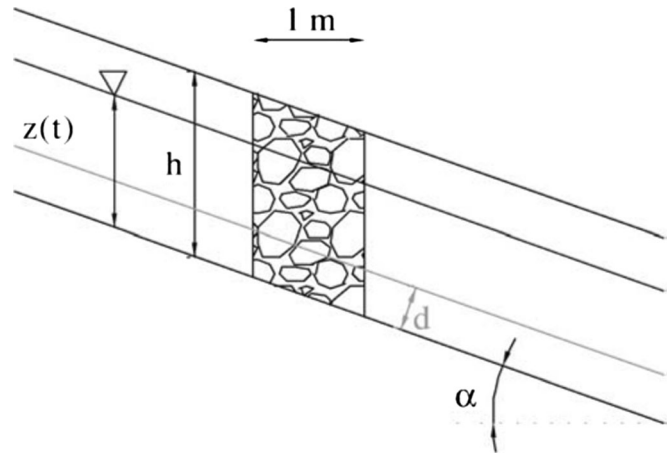

Fig. 2 Schematic representation and parameters of the viscoplastic model (from Herrera et al. 2009)

an input signal (e.g. rain and evapotranspiration) and an output signal (e.g. displacement velocity or water table level). This model has successfully been applied to Salazie cirque landslides in Reunion Island (Belle et al. 2013), permitting to predict deep-seated landslide movements and for studying their mechanism. The second model uses a simple 1D mechanical (MA) model which combines a simple 1D infiltration model and a viscoplastic rheology to take into account changes in pore water pressure. The third model (IRMA) is a combination of the previous ones; the IR model allows to obtain the groundwater level from the precipitation time series, and the viscoplastic model is applied using the computed groundwater level time series to predict the displacements.

The performance of different combinations of models is evaluated against the multi-parametric and multi-year dataset acquired at the Super-Sauze landslide (South East France), one of the
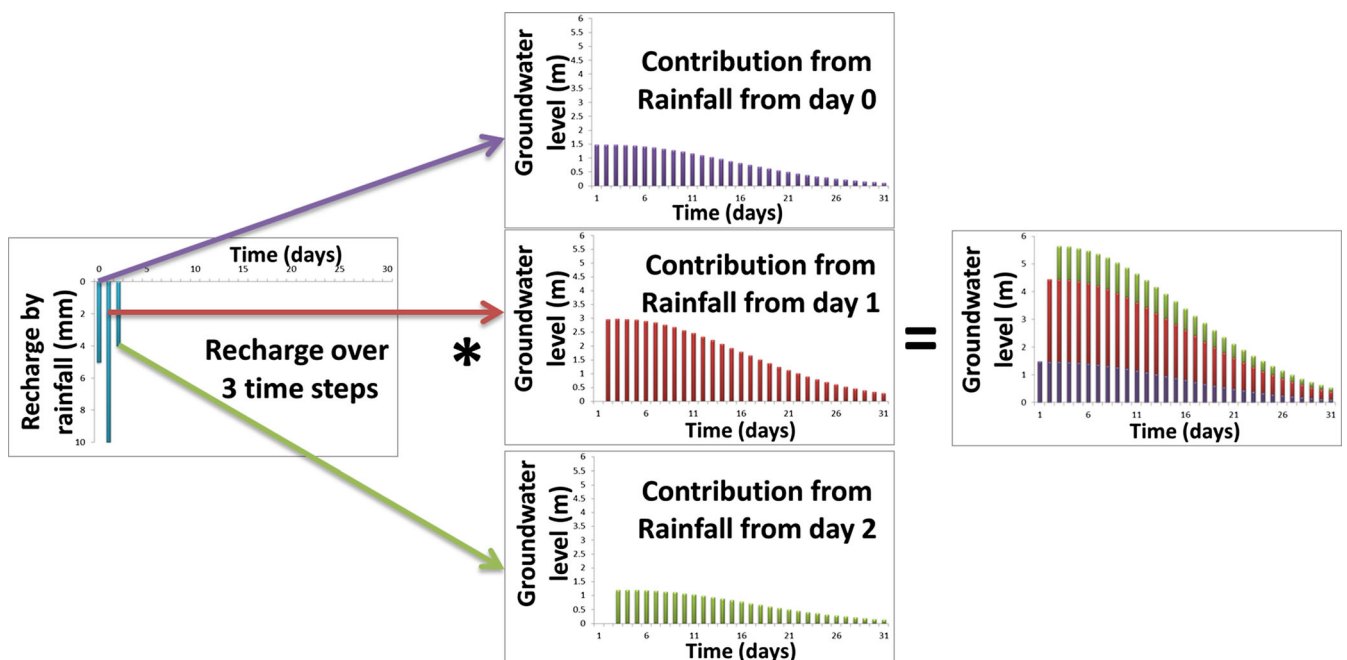
Fig. 1 Schematic framework of application of the impulse response (IR) model
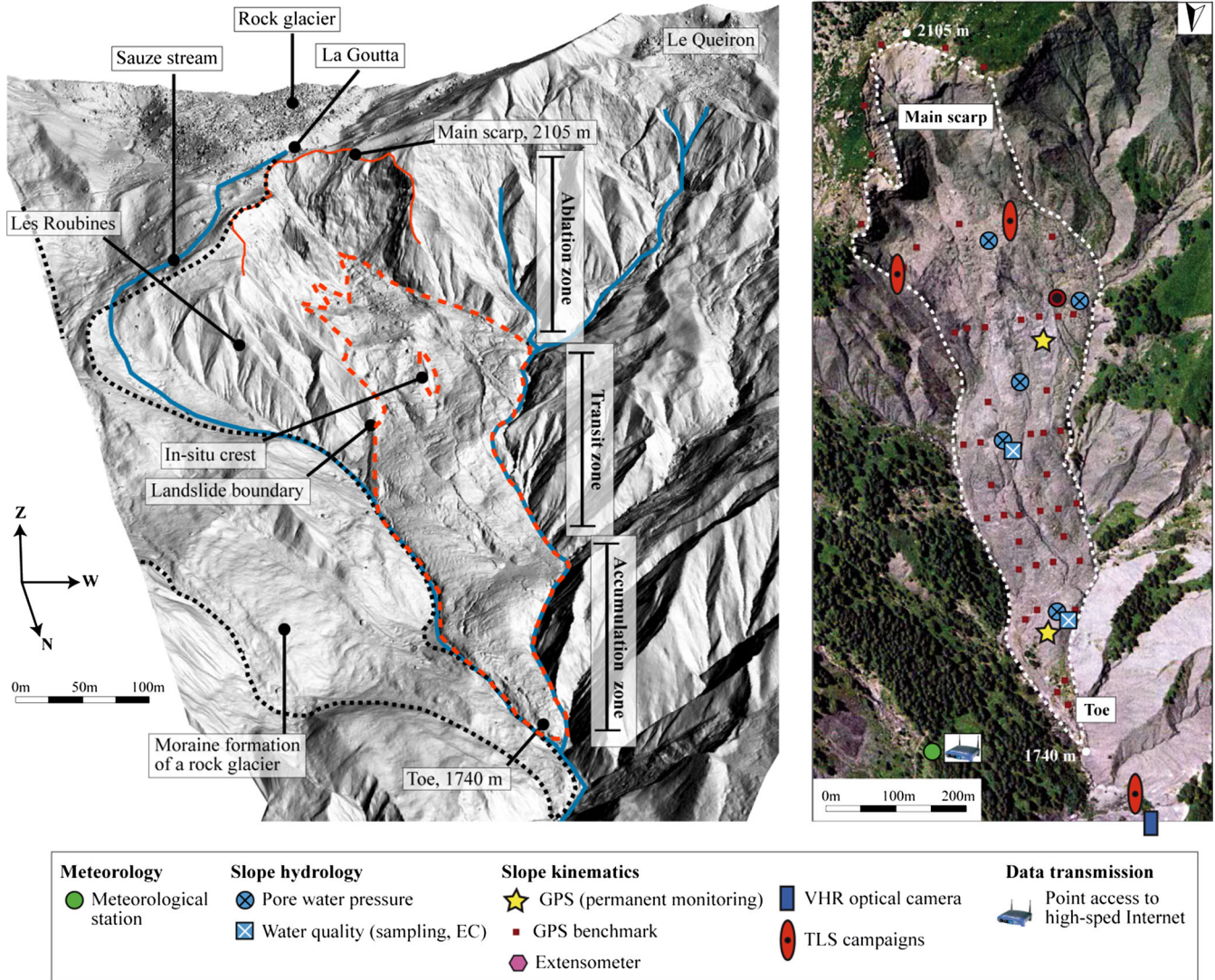
Fig. 3 The Super-Sauze Landslide Observatory; landscape represented on an airborne LiDAR point clouds (*left*) and position of the monitoring systems (*right*)

continuously active (with velocities from 0.001 to 0.4 m.day⁻¹) and instrumented clayey landslide in the European Alps.

Description of the forecasting models

Impulse response model—IR

The impulse response model (IR) is derived from the TEMPO modelling approach (Pinault and Schomburgk 2006), originally developed for the analysis of hydrogeological and hydrogeochemical time series and successfully tested for landslide analysis (Belle et al. 2013).

The IR model reproduces a discrete output signal S using the convolution product of a discrete input signal E by a transfer function G as described in Eq. 1 and illustrated in Fig. 1. The convolution is based on impulse response functions.

$$S(n \cdot dt) = \Gamma * E(t) = \sum_{i=1}^{k} \Gamma(i \cdot dt) \cdot E((n-i+1) \cdot dt) \quad (1)$$

where n is the discretized interval time, and k is the order (length) of the impulse response.

In the described methodology, the impulse response model is used for two purposes: (1) the prediction of the fluctuation of the water table due to the infiltration of water from rainfall and melting of the snow pack and (2) the prediction of the landslide velocity also based on the same water inputs.

The water is, indeed, the main driver of both the phenomena of interest. Therefore, the shape of the transfer functions (Γ) we used is a usual shape in hydrological modelling: i.e. the convolution of a Gaussian function by an exponential function.

$$\Gamma(t) = \exp\left(-\ln(2)\left(\frac{t-T}{D}\right)^2\right) * \exp\left(-t\frac{\ln(2)}{L}\right) \quad (2)$$

The three degrees of freedom to optimize are the following:

- $T \geq 0$—the lag in the response of the system after a rainfall event;
- $D > 0$—the duration of this response;
- L—the duration of the relaxation of the system
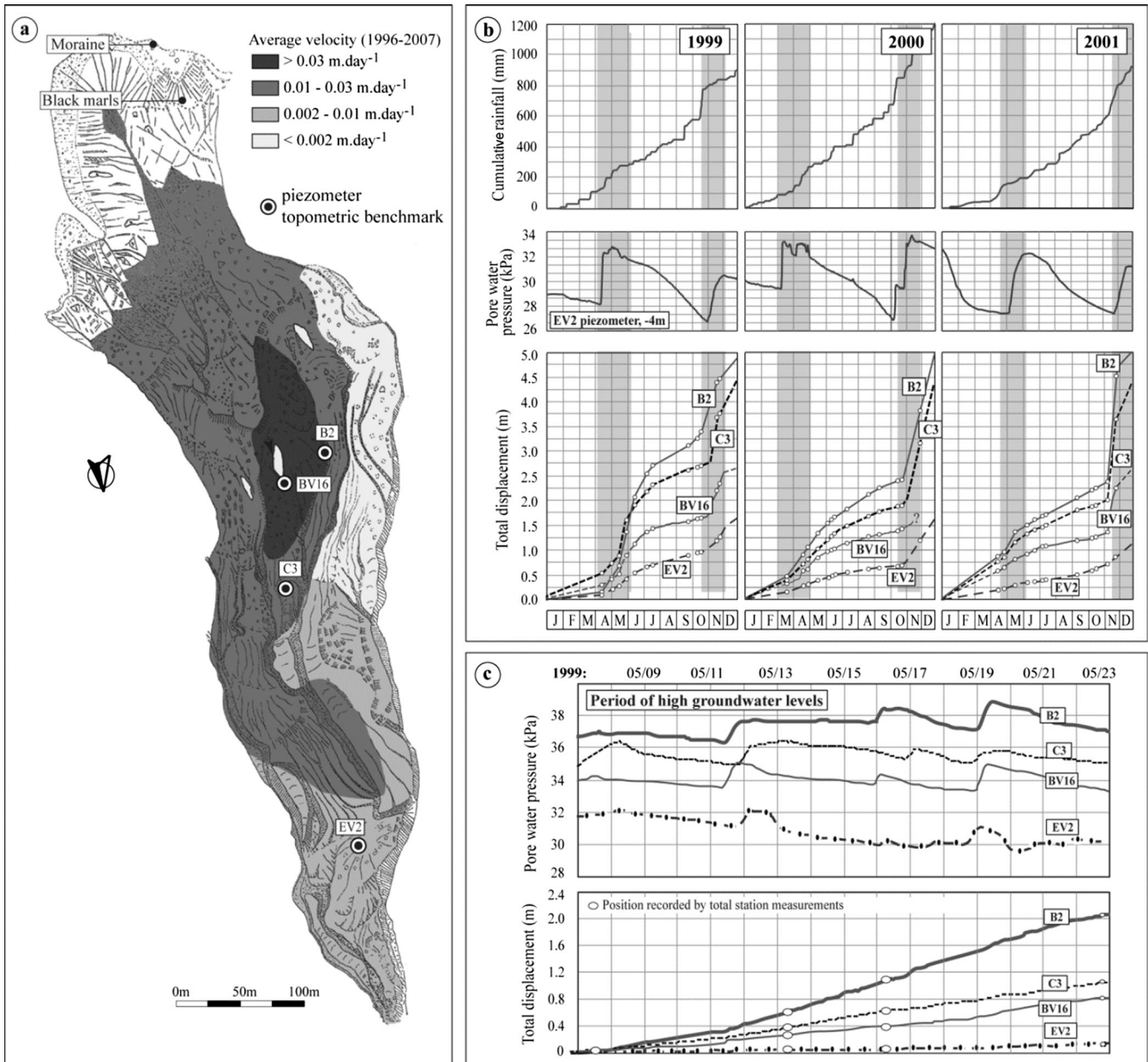
Fig. 4 Spatial and temporal kinematic pattern observed at Super-Sauze; average velocity field observed during the period 1996–2007 from a network of ca. 40 benchmarks (**a**); observed 'pore water pressure-displacement' pattern at the annual scale (**b**) and at the event scale for a period of high groundwater level in May 1999 (**c**)

Based on optimization and inversion techniques, the IR model is able to combine several types of input data (e.g. evapotranspiration, internal source input, snow melt water), thus allowing us to analyse the contribution of additional non-correlated entries to the model.

The relationships linking a single output time series S to several input data E_i are the following:

$$S = \beta \cdot \left(\sum_{i\gamma_i} (\Gamma_i * E_i(t)) + \text{cst} \right) \quad \text{with} \quad \sum_{i\gamma_i} = 1 \qquad (3)$$

Where β is a normalization constant, and γ_i and Γ_i, respectively, are the contribution coefficient and the transfer function of the input E_i, and cst, a constant corresponding to constant contribution.

To characterize the contribution of melting snow as water infiltration, a simple degree-day model has been used to create time series of melt water from precipitation and air temperature observations (Kustas et al. 1994). The model used in this work is based on simple parameters such as a critical temperature T_c (in °C) to characterize the quality of the precipitation (e.g. solid or liquid) and a coefficient a (in m.°C^{-1}.day^{-1}) which define the rate of snow melting (Eq. 4):

$$\begin{aligned} \text{Potential snowmelt} &= a \cdot (T(t) - T_c) \quad &\text{if } T(t) > T_c \\ \text{Potential snowmelt} &= 0 \quad &\text{if } T(t) < T_c \end{aligned} \qquad (4)$$

According to sensitivity analysis further described in the "Characteristics of the Super-Sauze Landslide Observatory"

Fig. 5 Observed daily precipitations (rainfall and snowfall) and cumulative displacements at position BV16
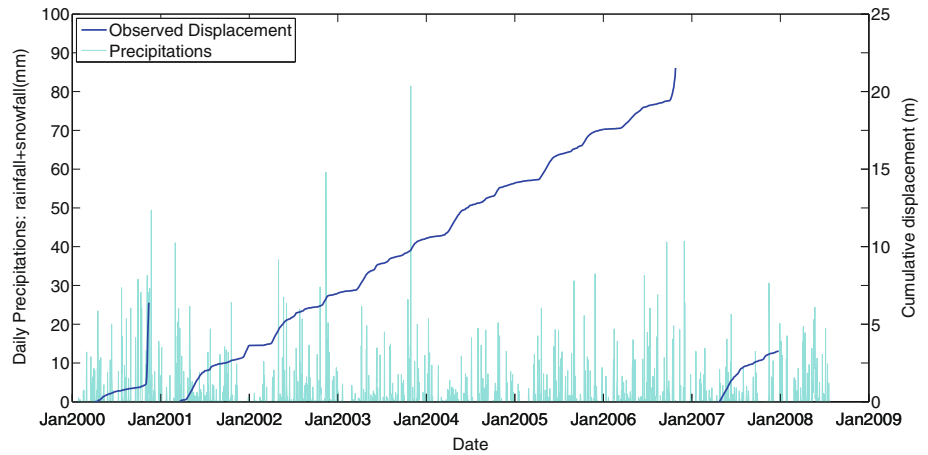
section, the inputs data used for the IR modelling of both phenomena (displacement velocities and fluctuation of water table level) are the rainfall and the melting of the snow pack. A supplementary water input, a source, is also considered, but as it can be assumed to be constant (see the "Characteristics of the Super-Sauze Landslide Observatory" section), it is integrated in the IR models as a constant (constant of Eq. 3).

Mechanical viscoplastic model—MA

A simple 1D mechanical model based on the theory of limit equilibrium of soil slopes and on a constitutive viscoplastic law is considered from Herrera et al. (2009). The model consists of two parts; the first part simulates the deformation of the mass and the displacement pattern and the second part simulates the variations in water table level and in pore water pressure. The model assumes a rigid body, with an infinite mass of thickness h, sliding over a pre-existing slip surface, characterized by an infinite slope, with a shear zone of thickness d and an inclination α (Fig. 2).

Assuming that a Mohr-Coulomb criterion and a Bingham model can be used to estimate, respectively, the resisting forces and a viscous force, the momentum equation along the slope direction is defined by Eq. 5:

$$\tau - \left[c + (\sigma_n - p_w(t)) \cdot \tan\phi \right] = \rho \cdot h \cdot a(t) + \frac{\eta}{d} v(t) \qquad (5)$$

where τ (in Pa) is the destabilizing shear stress, σ_n is the normal stress (in Pa), $\varnothing$ (in °) is the material friction angle, c (in Pa) is the material cohesion, ρ is the soil density (in kg.m^{-3}), η is the viscosity (in Pa.s^{-1}), d (in m) is the thickness of the shear zone, $p_w(t)$ (in Pa) is the pore water pressure as a function of time, $a(t)$ (in m.s^{-2}) is the acceleration as a function of time, and $v(t)$ (in m.s^{-1}) is the velocity as a function of time.

The evolution of the water inside the landslide is evaluated through two antagonist approaches: the increase in water level through infiltration and the evacuation of water through relaxation.

The daily effective precipitation amounts (e.g. water incoming either from rainfall or from snowmelt, as defined in §2.1) are used as direct inputs. Changes in groundwater level due to precipitations are supposed, in first instance, to be directly proportional to the effective rainfall intensity:

$$dz_{recharge} = \frac{I_{precipitation}}{n} \qquad (6)$$

where $I_{precipitation}$ is the effective precipitation (addition of rainfall with snowmelt, in mm^{-2}.day^{-1}), n is the material porosity and $dz_{recharge}$ the daily change in groundwater level due to water infiltration (in m).

Fig. 6 Observed 10- and 50-day cumulative rainfall amounts and date of fluidization events
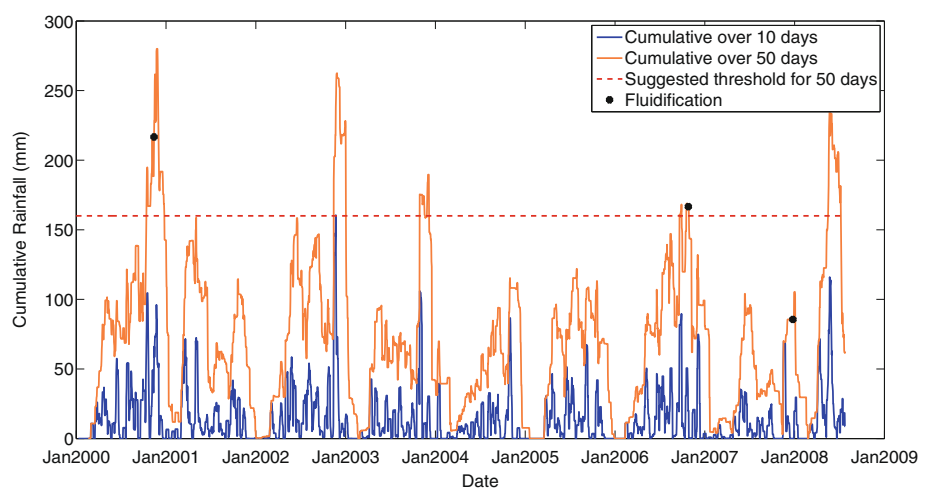
Fig. 7 Observed daily rainfall amounts and measured velocity at BV16 location for the period from January 2000 to January 2009
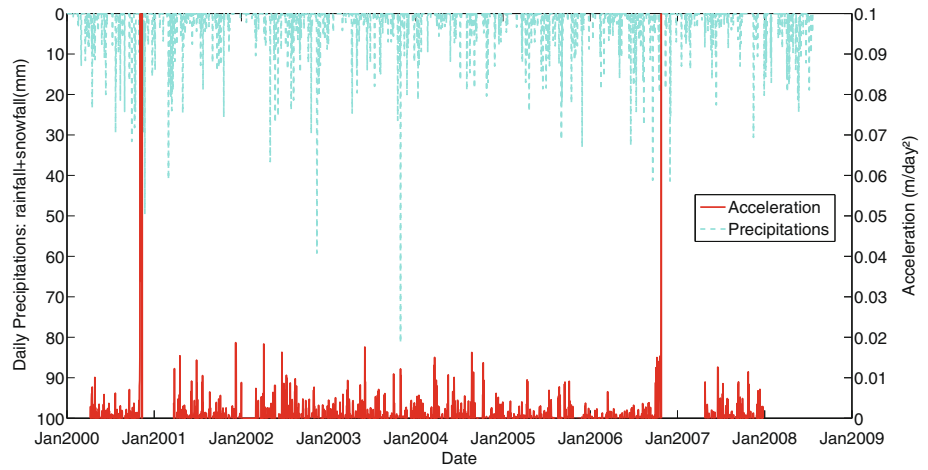
The dissipation of excess pore-fluid pressure in the saturated layer is computed using Terzaghi's one-dimensional consolidation theory (Eq. 7):

$$ep_w(t) = ep_{wo} \cdot e^{-k/T_v} \tag{7}$$

where ep_{wo} (in Pa) is the initial excess pore water pressure, k is the number of days since the last recharge and T_v (in day) is the time factor controlling the dissipation of the excess pore pressure.

With the assumptions of a groundwater flow parallel to the slope surface, the pore water pressure is defined by Eq. 8:

$$p_w = z(t)\gamma_w \cdot \cos^2 a \tag{8}$$

where $z(t)$ (in m) is the position of the groundwater level, and γ_w is the unit weight of water (in N.m^{-3}).

According to these assumptions, the initial excess pore water pressure (ep_{wo}) was estimated according to Eq. 9:

$$ep_{wo} = [z_{max}(t) - z_o] \cdot \gamma_w \cdot \cos^2 a \tag{9}$$

where $z_{max}(t)$ is equal to the highest groundwater level since the last recharge (i.e. since the last time the effective rainfall has been positive), and z_o is the groundwater when the landslide is at rest.

Hence, the variation of the pore water pressure is given by Eq. 10 and the variation of water table level by Eq. 11:

$$\Delta p_w = \Delta p_{w,recharge} + \Delta p_{w,dissipation} = \frac{I_{precipitation}}{n} \cdot \gamma_w \cdot \cos^2 \alpha + ep_{wo} \cdot e^{-\frac{k}{T_v}} \cdot \left(1 - e^{\frac{1}{T_v}}\right) \tag{10}$$

$$\Delta z = \Delta p_w \gamma_w \cdot \cos^2 \alpha \tag{11}$$

The displacements are then computed by solving Eq. 5 using sequential quadratic programming algorithms (SQP) (Boggs and Tolle 1996) to optimize some parameters, among

geometry parameters (h, d) and material properties (ρ, ϕ, η, n, T_v). The choices of the parameters to be optimized as well as the range values chosen for the optimisation, are discussed in the "Characteristics of the Super-Sauze Landslide Observatory" section.

Fig. 8 Observed and computed cumulative displacements with the three models
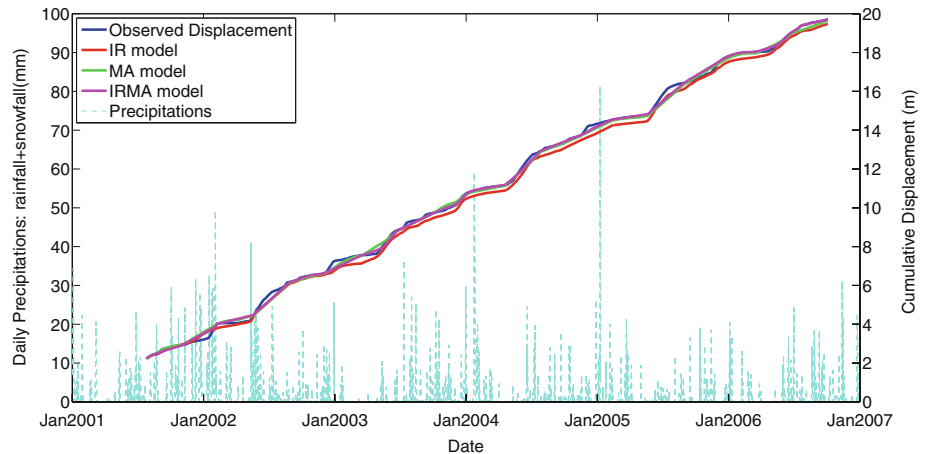
Coupled statistical-mechanical (IRMA) model

This model combines the IR and MA models. The IR model is used to simulate groundwater level from the time series of observed rain and temperature; then the mechanical part of the MA model is used to compute the displacement rate of the landslide directly from the computed groundwater levels converted into pore water pressure.

Characteristics of the Super-Sauze Landslide Observatory

The Super-Sauze landslide is located in the French South Alps (Barcelonnette Basin) and is continuously active since its triggering. The landslide is typical of flow-type gravitational processes developed in Callovo-Oxfordian clay shales (e.g. called black marls in the region). In the mid-1960s, the upper part of the Sauze torrential catchment was affected by rock failures along preexisting lithological and tectonic discontinuities. The failed material was composed of rocky panels progressively transformed into a silty-sandy matrix. During successive weathering cycles, the matrix has been altered resulting in marly fragments of heterogeneous sizes. From the 1970s until today, the landslide material has been gradually filling the thalweg (Fig. 3). In 2007, the landslide extents over a distance of 920 m between an elevation of 2,105 m at the scarp and 1,740 m at the toe with an average width of 135 m and an average slope of 25°. The total volume is estimated at 560,000 m^3 (Travelletti and Malet 2012). The landslide consists of two vertical units: the upper unit (5 to 10 m thick) is a moderately stiff and semi-permeable material, while the second unit (with a maximum thickness of 10 m) is a stiff and impervious material (Malet and Maquaire 2003). A slip surface of 5 to 10 cm thick is separating these two landslide units, as it was evidenced from inclinometer measurements and observation of borehole samples (Malet and Maquaire 2003). Detailed information on the hydrological and geomechanical properties of this low plasticity and intensely fissured reworked material can be found in Malet (2003). These two landslide units overlay a bedrock of intact clay shales.

The landslide is part of the French Multidisciplinary Observatory of Versant Instabilities (OMIV) which aims at acquiring and distributing multi-parameter observations on different types of landslides through geomorphologic, geologic, hydrologic, geophysical and seismological long-term monitoring. In this context, the kinematics of the landslide is currently monitored by differential Global Positioning System (campaigns and permanent receivers), terrestrial laser scanning (TLS) surveys, remote very high-resolution cameras and an extensometer (Travelletti and Malet 2012).

Pore water pressures are monitored automatically in four piezometers (B2, BV16, C3 and EV2; Fig. 4a) which are installed at −4 m in depth with the top of the filter zone at −3 m sealed with bentonite plugs. The high displacement rates require installation of new piezometers approximately every 2 years at the same location to monitor the hydrological features of the landslide over long periods.

Meteorological parameters are monitored on the East part of the landslide, at a distance of about 500 m (Fig. 3). The maximum observed daily precipitation for the period 1999–2010 reaches 81.4 mm.day^{-1}, and the yearly total amount has important variability ranging from 540 to 935 mm.year^{-1} (Fig. 5).

Table 1 Mean values of statistical criteria for the optimization of the IR, MA and IRMA models

Prediction	Optimized calibration		
	IR model	MA model	IRMA model
RMSE (m.day^{-1})	0.0043	0.0053	0.0049
Nash	0.4892	0.2037	0.2812

The deformation pattern is controlled by changes in the vertical position of a perennial groundwater table resulting in the development of positive/negative pore water pressure in the moving material. These groundwater level fluctuations are controlled by flow in the soil matrix and flow in large cracks and by in-depth recharge from the torrents or from uphill springs bordering the landslide (Malet et al. 2005; de Montety et al. 2007).

The displacement pattern is spatially heterogeneous (Fig. 4a); the landslide is characterized by zones with different velocities (0.001 to 0.03 m.day^{-1}) according to the underlying bedrock geometry and the average position of the groundwater level (Travelletti and Malet 2012). Accelerations with velocities up to 0.4 m.day^{-1} may be observed each spring season (Fig. 4b). Displacements are mainly parallel to the dip direction of the slope.
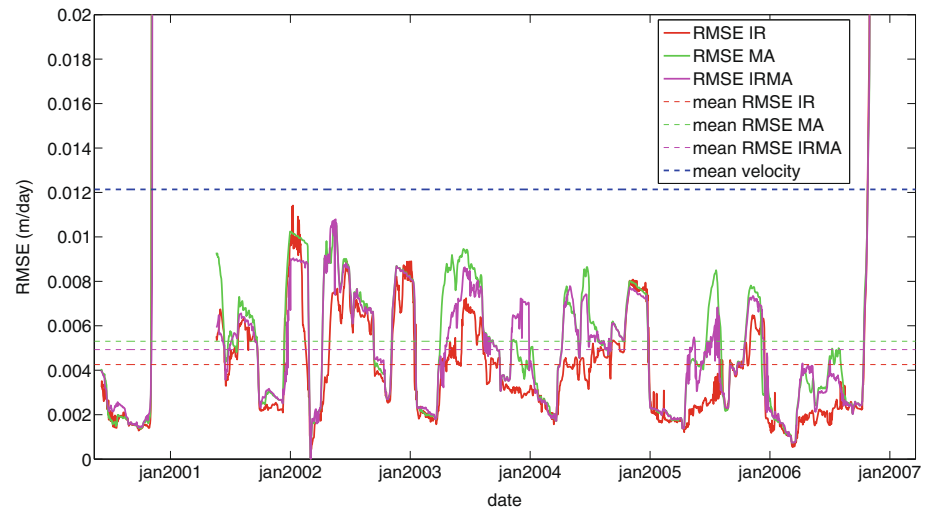
As an example, Fig. 4 shows the 'pore water pressure-displacement' pattern at the annual (Fig. 4b) and event scales (Fig. 4c) at several locations, for the period 1997–2001. Landslide fluidization events have also been observed with velocity larger than 1 m.min^{-1}; such as in 1999, 2001 and 2006 (van Asch et al. 2006).

The analysis focuses on the displacement time series of the location BV16 (Figs. 4b and 5) which corresponds to the most active part of the landslide; at that position, displacements are measured in continuous by a wire extensometer (Malet et al. 2002), the total displacements observed for the period 1999–2010 reach more than 20 m (Fig. 5). The data displacements have been previously smoothed to avoid negative displacement velocities. When looking at the relationship between precipitations and landslide velocities, landslide velocities appear to be more influenced by cumulative amounts of precipitation over several days than maximum daily rainfall. For instance, the November 1st, 2003 heavy rainfall triggered neither acceleration of the mass nor a fluidization event (Fig. 7). Moreover, when analysing the 10- and 50-day cumulative rainfall amounts (Fig. 6), we observe that fluidization events occur once the cumulative rainfall reaches more than 160 mm. However, this threshold is not enough to predict fluidization of the landslide. It has been overpassed several times without any changes in the displacement regimes of the landslide.

Table 2 Values of the viscoplastic model

Fixed parameters	Values	Optimized parameters	Range of value
α	25°	T_v	4–400 days
g	10 m·s^{-2}	n	0.001–0.59
d	0.2 m	ϕ	18°–35°
c	14 kPa	ρ	16–24 kN·m^{-3}
h	9 m	η	10^8–$3\ 10^{11}$ Pa·s

Before the occurrence of a fluidization event, the velocity of the mass increases (Fig. 7). Compared with the evolution of the velocity modelled with the changes in pore water pressure, these indicators could provide some rigorous criteria to forecast the possible occurrence of a fluidisation event.

Validation of the methodology: model calibration and performance evaluation

The objective of the model application is to predict daily displacement from the precipitation time series. Therefore, the calibration procedure has been performed on a daily basis by optimizing model performance over several sizes of time windows. The used optimization algorithm is the SQP method (sequential quadratic programming) (Boggs and Tolle 1996) which is adapted to the optimization of non-linear dynamic systems. Several parameters have to be optimized with this procedure:

– For the IR model, for each time series of input (i.e. rainfall and snow melt) the parameters T, D and L of the transfer function are optimized. The respective contributions of these input components (γ_i) as well as the coefficient β (defined in the "Impulse response model—IR" section) are also optimized. So, in the case of two input data (rainfall and snow), eight parameters have to be optimized (T_1, D_1, L_1, T_2, D_2, L_2, β, γ_1).

– For the MA model, the choice of the parameters to be optimized depends on the knowledge of the parameters for the specific site. For instance, in the case of the Super-Sauze landslide and taking into account the outcomes of the sensitivity analysis, six parameters are optimized, namely ϕ, ρ, η, n, T_ν and h while the other parameters are considered constant.

Indeed, the value of the parameters α and c are well established in this site, thanks to in situ measurements (Spickermann et al. 2009; van Asch and Malet 2009). The parameters d and h are directly related to η and ρ in Eq. 5, so it is also fixed. Concerning the parameters ϕ, ρ, η, n and T_ν, the range value for each of them has been determined depending on the uncertainty of the values and on the value which can be found in the literature. Thus, the range for ϕ corresponds to the interval of uncertainty on the site; for η and T_ν, large ranges have been considered as reported in different studies from the literature. For the IRMA model, the same parameters of the IR model are optimized, including also the z_{max} (defined in the "Mechanical viscoplastic model—MA" section) and the adequate parameters of the mechanical part of the MA model, so in this case ϕ, ρ and η.

The three models have been applied to the complete period (01/01/1999–31/10/2006). A first validation of the model is performed over 100-day successive periods. The different models are calibrated over periods of 100 days, displacements velocities are computed on the same periods and then compared with the observed displacements (Fig. 8). We can see that the cumulative displacements computed by the three models fit the observed data with a very good accuracy. The difference of values between observed and calculated displacements is lower than 49 cm. The IR and the IRMA models reproduce more precisely the short time variations of displacements, whereas the MA model smooths the observed data.

Various tests have been conducted to improve this model by the integration of additional input data such as evapotranspiration (calculated using the Penman-Monteith equation), the delay due to snow accumulation and melting, the precipitation typology
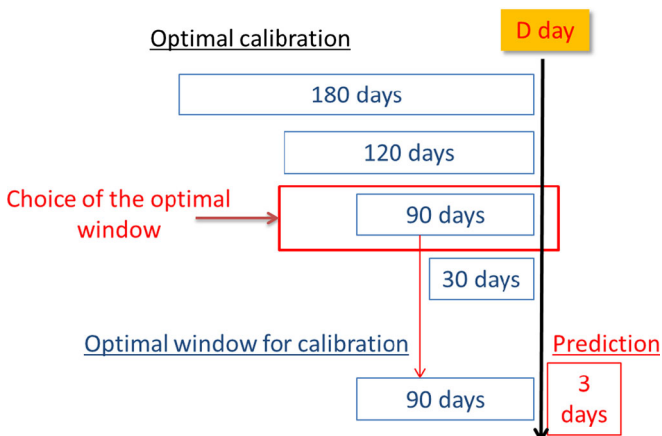
Fig. 10 Schematic framework of the forecasting procedure

Fig. 11 Predicted and observed cumulative displacements
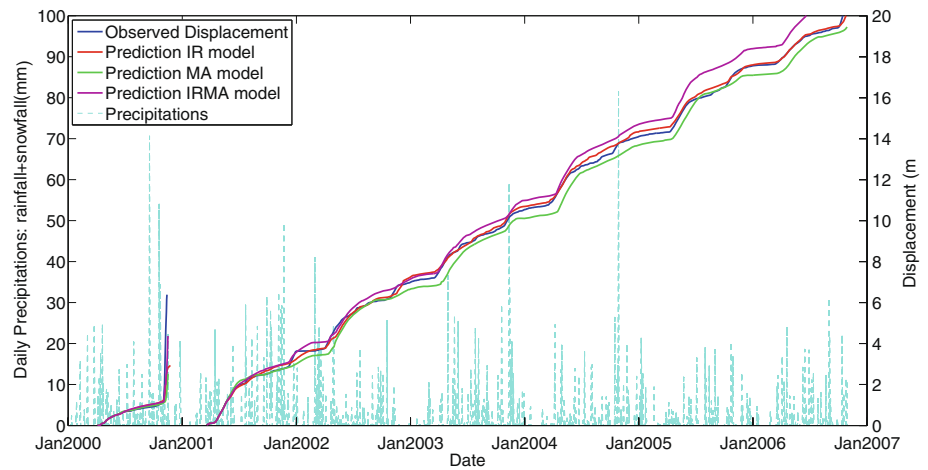
(liquid/solid) and the discharge of uphill and lateral springs. The most accurate model is that considering two distinct impulse responses (e.g. one for the rainfall, one for the snow) and integrating the contribution of a source bringing a constant equivalent of water fluxes of 10 mm.day⁻¹.

The models are then tested for any day of the period of interest. Before a given day D, an optimal calibration window size among a period of 60 and 180 days is looked for. Results indicate that most of the optimized windows are around 100 days. Then the model is calibrated, and the displacements are computed on this period. The next day of calibration is then shifted at $D+1$, and the procedure is iterated. For the MA model, the parameters are optimized within the range values detailed in Table 2.

The performance of the model is evaluated with the Nash and RMSE (Root Mean Square Error) statistical criteria to measure both the ability of the model to reproduce the finest evolutions and the global tendency (Fig. 9 and Table 1). The IR model provides variable but generally good accuracy, with Nash values ranging from 0.07 to 0.96 and RMSE values from $5.7 \ 10^{-4}$ to 1.10^{-2} m.day⁻¹ (Fig 9). The mean value of RMSE is $4.3.10^{-3}$ m.day⁻¹, and the mean value of Nash is 0.49 which indicate a good quality model (Table 1).

The MA model and the IRMA model also provide good results with, respectively, a mean Nash value of 0.20 and a mean RMSE value of $5.3 \ 10^{-3}$ m.day⁻¹ and a mean Nash value of 0.28 and a

mean RMSE value of $4.9 \ 10^{-3}$ m.day⁻¹ (Table 1). The accuracy of the models suggests the possibility of applying the three models as a forecasting tool.

### Application of the methodology: model prediction

The three models are then applied as potential forecasting tools using the framework described in Fig. 10.

In order to test the ability of the methodology to be used in an operational early warning system delivering daily warnings in near real time, a prediction procedure has been developed and tested. The method has been applied as if the new data were received each morning and processed in real time on a daily basis.

Hence, for each day, the "new" received data are added to the historical time series. The calibration is performed over time windows of different durations (Fig. 10). The optimal calibration is then used to predict the displacement for the three following days, based on the meteorological data of these three next days, assumed to be meteorological forecasts. The procedure is then repeated for the next day, with a complete new calibration.

In order to test the 3-day prediction procedure, the daily predicted displacements are compared with the observed displacements for the three predicted days. With this approach, the IR model provides the best predicted displacements; the IRMA model overestimates the displacement for the second part of the curve, and the MA model slightly underestimates the displacements

Fig. 12 Predicted velocity for the three models (IR, MA and IRMA)
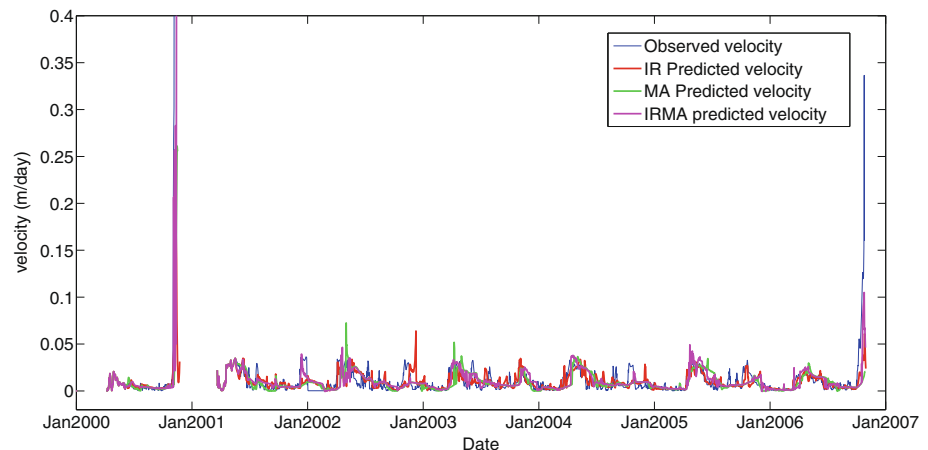
Fig. 13 Predicted velocity from September 2001 to January 2003
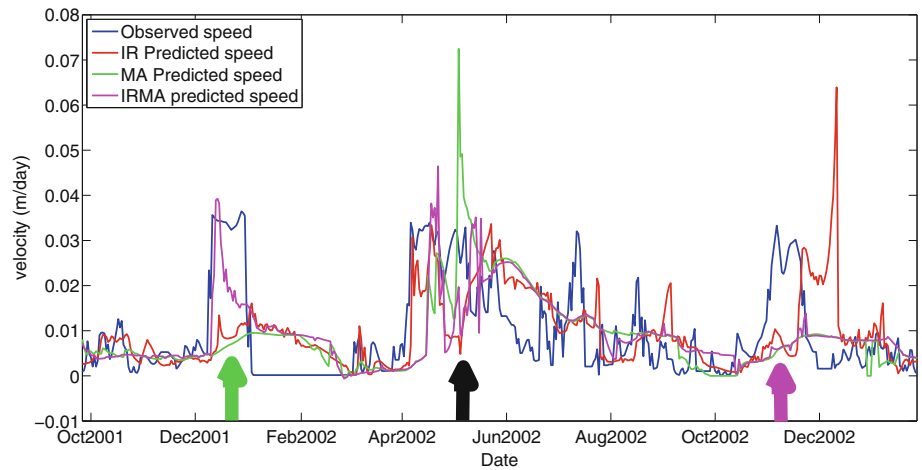
(Fig. 11). These results suggest that the models are adapted to predict the movements (cumulative displacements and displacement velocities) for the three following days (Fig. 12).

However, for other periods, some discrepancies between the model and the observations exist (Fig. 13); for instance, the models underestimate the displacement rates in December 2001 (green arrow), resulting in a shift in the displacement. In December 2002 (pink arrow), the IR model is delayed, resulting in a delay in the computed cumulative displacement.

Based on these results, it is then necessary to find rigorous criteria and thresholds for predicting the occurrence of a catastrophic fluidization event. The inverse velocity criterion is analysed as it has been already applied in other studies (Petley et al. 2005, 2002; Rose and Hungr 2007). The analysis of the evolution of the inverse velocity (Fig. 14) indicates that this parameter is not suitable for predicting the occurrence of fluidization, as this parameter has been found to decrease, even if no fluidization phenomenon occurs.

Another approach consists in analysing the evolution of some parameters which are optimized each day according to the MA model. In particular, it is interesting to focus on the evolution in

time of the consolidation time (Fig. 15) and the viscosity (Fig. 16). It appears that the consolidation time strongly decreases during the period preceding the occurrence of a fluidization event (from 01/11/2000 to 13/11/2000 and from 21/10/2006 to 31/10/2006) as well as the viscosity largely increases at that time. However, this trend can also be observed when no fluidization event has occurred. Thus, these criteria are not suitable for predicting statistically a fluidization event. During the period preceding the occurrence of a fluidization event, the model is not able to reproduce the displacement with a good accuracy. Indeed, the RMSE criterion computed on the three predicted days largely increases, as can be observed on Fig. 17, possibly indicating an important change in the mechanical behaviour and kinematic regime of the landslide. Moreover, the large increase of this criterion appears only before the occurrence of a flow (Fig. 18). This result suggests that the RMSE variation could be a good indicator of the occurrence of a fluidization event several days before the occurrence of the event itself.

It is essential to propose rigorous thresholds for predicting the occurrence of a catastrophic fluidization event. The two first proposed thresholds are based on the normal law distribution of the RMSE values, with the use of a threshold equal to the mean of

Fig. 14 Evolution of the observed velocity over time
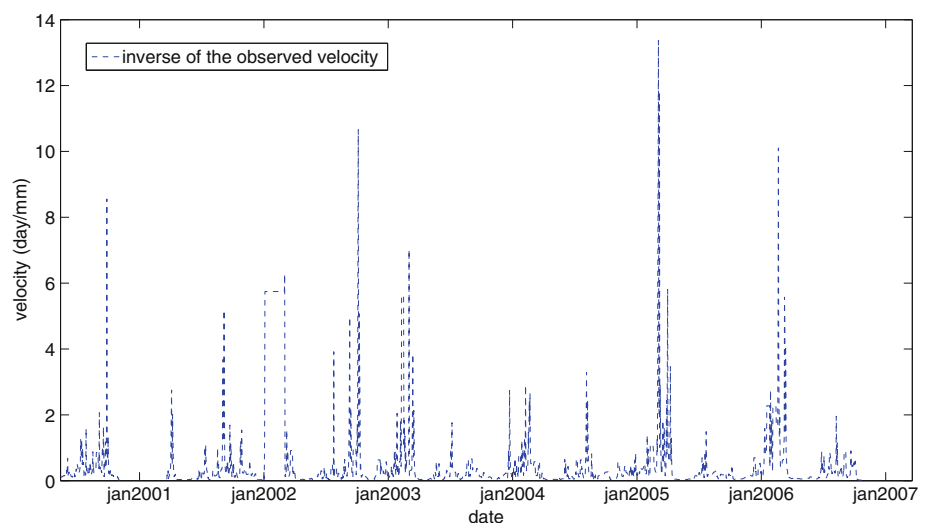
Fig. 15 Evolution of the consolidation time parameter over time
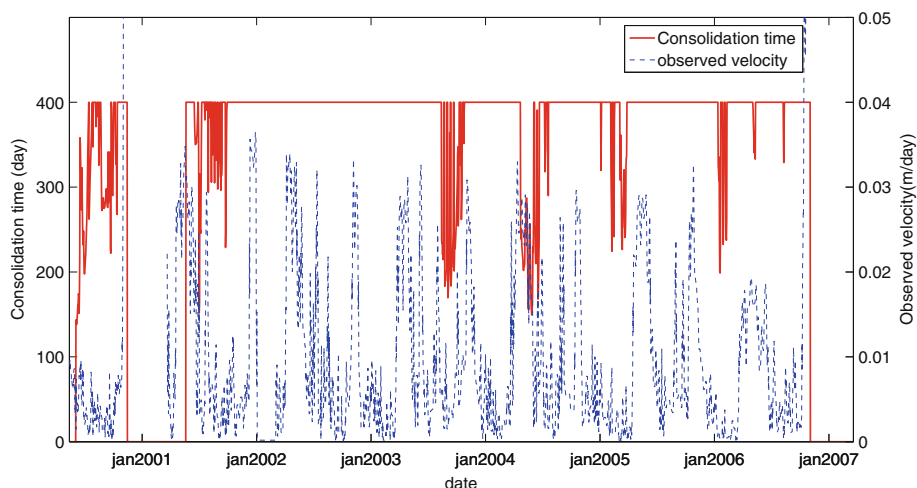
the RMSE plus three standard deviation values of the RMSE and the second one equal to the mean of the RMSE plus one standard deviation values of the RMSE:
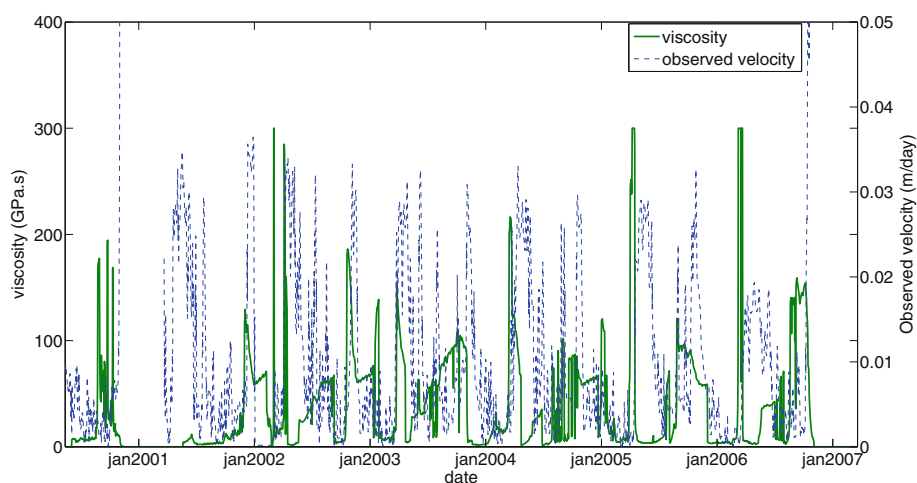
$$t1a = mean(x) + 3\sigma_x \tag{12}$$

$$t1b = mean(x) + \sigma_x \tag{13}$$

A third threshold is defined based on the curve detailed on Fig. 19 where the RMSE values are sorted. The threshold is then chosen at the curve limit between the low and the high values, at the point of maximum curvature of the distribution.

These thresholds are proved not only to be efficient both to predict the occurrence of the fluidization for the study case but also not to launch false alarm. The threshold based on the point of maximum curvature is not considered further in the study in order to reduce the approximation which might be present when determining where the maximum curvature is.

Finally, the advance in alert before the occurrence of the flow is analysed on the RMSE values for the two selected thresholds and for the three models. They are compared to thresholds computed on the basis of the observed displacement rates with the same three criteria (Table 3).

The first conclusion is the dependency of the results on the analysed fluidization events. Indeed, the delay provided by the IR model with threshold $t1$ is 11 days for the event in 2000 and 3 days for the event in 2006. As already suspected, the threshold $t1b$ provides better delays with an alert given between 10 and 19 days before the occurrence of the event. Regarding the performance of the models, the MA gives the worst results, whereas the coupled model provides the best results when analysing the two fluidization events.

With the two proposed thresholds, no false alarms would have been raised during the study period, and also, no fluidization event would have been missed. Therefore, in view of these results, based on a limited period of time, the two proposed thresholds remain potential good candidates for the early warning system.

Discussion and conclusions

The capability to predict the complex displacement pattern (acceleration, deceleration) of landslide is an important issue for early warning. Most of the current alarm systems are based on simple criteria, such as cumulative precipitation thresholds, which can provide false alarms and make them therefore unreliable for people.

A methodology has therefore been tested to combine meteorological observations with statistical and mechanical models to

Fig. 16 Evolution of the viscosity parameter of the MA model over time

**Fig. 17** Observed displacement and RMSE computed before the flow
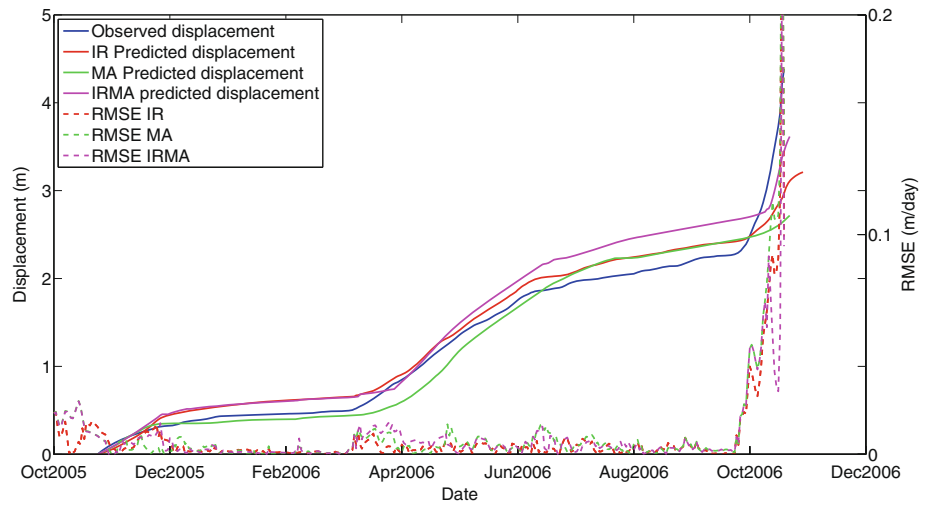
simulate the kinematic of landslides in their normal regime. The three proposed models demonstrate their capability to reproduce the landslide movements in regular situation, but not during fluidization events. Hence, these expected changes in the model-

ling capacities of the models make some good criteria to predict the acceleration of the landslides.

Furthermore, the use of models based on different approaches, statistical and mechanical, ensures their complementarity. If one

Fig. 18 Predicted RMSE and thresholds for the IR
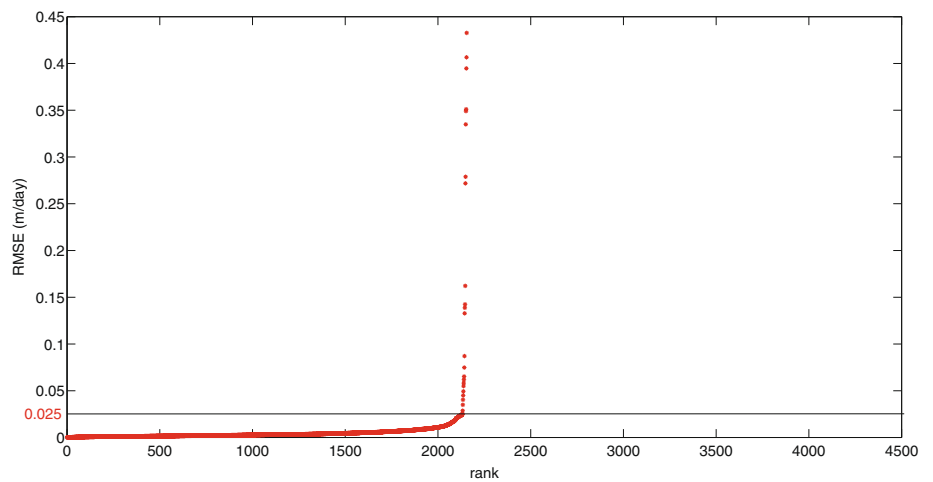
Fig. 19 Distribution of the predicted RMSE for the IR. The threshold (maximum curvature) is 0.025 m×day^{-1}
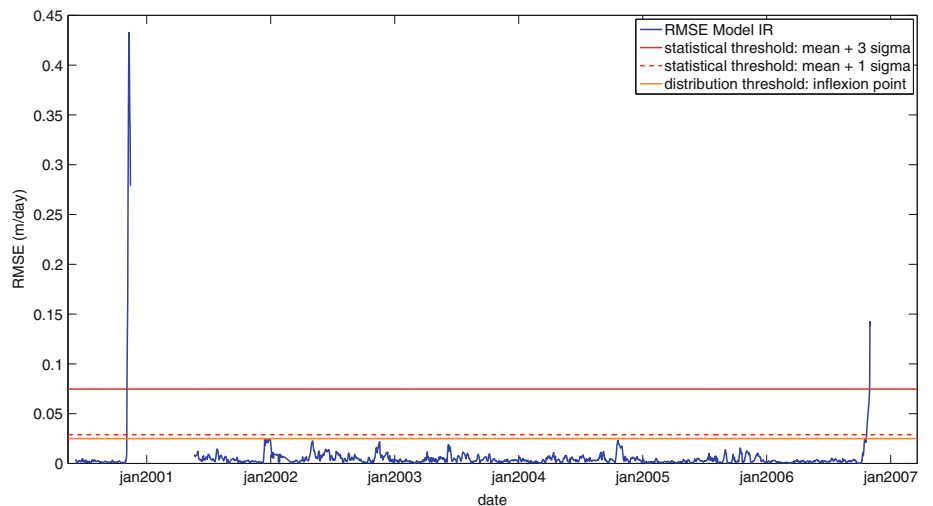
Table 3 Delay of alert before the occurrence of the flow

Delay in day	2000 flow/t1a (3sigma)	2000 flow/t1b (1sigma)	2006 flow/t1a (3sigma)	2006 flow/t1b (1sigma)
Observed velocity	11	11	7(3)	19(13)
IR	11	11	3	11
MA	11	11	2	11
IRMA	8	9	10	19

of the models would exhibit weaknesses in a specific context, the other models are likely not to have the same deficiency. For example, if at one site, piezometric levels are not available, the IR and the direct precipitation-velocity MA models should be applied, whereas the other IRMA model, as less constrained, should be less effective.

The availability of data for early warning systems is a critical point. For this tool, long (at least 60 days) time series of both displacement and meteorological parameters are required. For prediction purposes (e.g. early warning), the data should be provided on a regular basis, with reduced uncertainties.

Due to the particular conditions featuring the mountainous environment and the dynamic of the object of study, most of the data should be pre-processed. Snow thickness measures are often lacking, and snow accumulation and additional water input due to snow melting should often be assessed through empirical relationships (e.g. solution of degree-day adopted in our tool). Meteorological observations and predictions could also refer to a station which is not located close to the monitored landslide. Hence, hypothesis should be made to estimate the meteorological conditions for the site, looking for homologue stations, where climate features are likely to be similar. Even in this case, corrections should be brought to take into account effects of elevation and exposition on temperature and precipitations. Displacement data are also likely to contain some noises that should be removed before the computation of the landslide velocities required to calibrate the models. In the presented case, the historical displacement data have been previously smoothed, using averaging and interpolation strategies. However, these techniques would not work for data acquired in real time.

Another question raised by the approach is the selection of the most pertinent thresholds. The use of statistical criteria (either the ones based on moment values or the ones on distribution shapes), even if objective and robust, could depend on the length of the dataset.

The proposed tool has proven to be valuable for the case study, with the aforementioned assumptions, and for the specific studied period, during which two fluidization events happened. In order to extend the methodology and to make it a potential generic warning system, it would however be necessary to test it on other sites to assess, for example, the potential influence of other geomorphological contexts or climatic patterns (such as the absence of snow) on the validity of the methodology.

The methodology could be applied through an automatic tool, which would collect on a regular basis meteorological and displacement data on external dedicated servers. The time resolutions of the models could then be adapted to the conditions of the landslides. For example, a daily analysis would be performed on a daily basis, but when thresholds would be passed, and warnings sent, a finer resolution (up to hourly basis) could be adopted.

This type of approach, quite innovative, would help to gather sufficient information from different sources of information (slope monitoring, model simulations) in order to find out if and when a slope is approaching collapse and to reduce the uncertainties (e.g. heuristic experience of the expert) in the assessment.

References

Angeli MG, Buma J, Gasparetto P, Pasuto A (1998) A combined hydrology/stability model for low-gradient clay slopes in the Italian Dolomites. Eng Geol 49:1–13

Belle P, Aunay B, Bernardie S, Grandjean G, Ladouche B, Mazué R, Join JL (2013) The application of an innovative inverse model for understanding and predicting landslide movements (Salazie cirque landslides, Reunion Island). Landslides. doi:10.1007/s10346-013-0393-5

Boggs PT, Tolle JW (1996) Sequential quadratic programming. Acta Numer 4:1–51

Caine N (1980) The rainfall intensity—duration control of shallow landslides and debris flows. Geogr Ann Ser A-Phys Geogr 62(1–2):23–27

Calvello M, Cascini L, Sorbino G (2007) A numerical procedure for predicting rainfall-induced movements of active landslides along pre-existing slip surface. Int J Numer Anal Methods Geomech 32:327–351

Cancelli A, Nova R (1985) Landslides in soil debris cover triggered by rainstorms in Valtellina (central Alps - Italy). Proceedings of the 4th International Conference and Field Workshop on Landslides, 267–272

Capparelli G, Tiranti D (2010) Application of the MoniFLaIR early warning system for rainfall-induced landslides in Piedmont region (Italy). Landslides 7:401–410

Capparelli G, Versace P (2010) FLaIR and SUSHI: two mathematical models for early warning of landslides induced by rainfall. Landslides 8:67–79

Corominas J (2000) Keynote lecture. landslides and climate. In: Bromhead EN, Dixon N, Ibsen M-L (eds) Landslides in research, theory and practice: proceedings of the 8th International Symposium on Landslides. Thomas Telford, Cardiff

Corominas J, Moya J, Ledesma A, Lloret A, Gili JA (2005) Prediction of ground displacements and velocities from groundwater level changes at the Vallcebre landslide (Eastern Pyrenees, Spain). Landslides 2:83–96

De Montety V, Marc V, Emblanch C, Malet J-P, Bertrand C, Maquaire O, Bogaard TA (2007) Identifying origin of groundwater and flow processes in complex landslides affecting black marls: insights from an hydrochemistry survey. Earth Surf Proc Landf 32(1):32–48

Eberhardt E (2008) The role of advanced numerical methods and geotechnical field measurements in understanding complex deep-seated rock slope failure mechanisms. Can Geotech J 45(4):484–510

Flageollet J-C (1996) The time dimension in the study of mass movements. Geomorphology 15:185–190

Fukuzono T (1990) Recent studies on time prediction of slope failure. Landslide News 4:9–12

Greco R, Giorgio M, Capparelli G, Versace P (2013) Early warning of rainfall-induced landslides based on empirical mobility function predictor. Eng Geol 153:68–79

Guzzetti F, Peruccacci S, Rossi M, Stark CP (2007) Rainfall thresholds for the initiation of landslides in central and southern Europe. Meteorog Atmos Phys 98(3–4):239–267

Guzzetti F, Peruccacci S, Rossi M, Stark CP (2008) The rainfall intensity duration control of shallow landslides and debris flows: an update. Landslides 5(1):3–17

Herrera G, Fernandez-Merodo JA, Mulas J, Pastor M, Luzi G, Monserrat O (2009) A landslide forecasting model using ground based SAR data: The Portalet case study. Eng Geol 105:220–230

Hutchinson JN (2001) Landslide risk—to know, to foresee, to prevent. Geol Tec Ambient 9:3–22

Intrieri E (2012) Design and implementation of landslide Early Warning Systems. PhD Thesis Manuscript, University of Florence, 216p

Kawamura K (1985) Methodology for landslide prediction. Proceedings of the 11th International Conference on Soil Mechanics and Foundation Engineering, San Francisco (California), 12–16 August 1985. Editor: Publications Committee of the ICSMFE, Balkema, Rottterdam, 3, 1155–1158

Kustas WP, Rango A, Uijlenhoet R (1994) A simple energy budget algorithm for the snowmelt runoff model. Water Resour Res 30(5):1515–1527

Larsen MC, Simon A (1993) A rainfall intensity-duration threshold for landslides in a humid-tropical environment, Puerto-Rico. Geogr Ann Ser A-Phys Geogr 75(1–2):13–23

Malet JP (2003) Les "glissements de type écoulement" dans les marnes noires des Alpes du Sud. Morphologie, fonctionnement et modélisation hydro-mécanique. PhD Thesis manuscript, Université Louis Pasteur, Strasbourg, 394p

Malet J-P, Maquaire O (2003) Black marl earthflows mobility and long-term seasonal dynamic in southeastern France. In Proceeding of the 1st International Conference on Fast Slope Movements, Naples, Italy, Patron Editore, Bologna, 333–340

Malet J-P, Maquaire O, Calais E (2002) The use of global positioning system techniques for the continuous monitoring of landslides: application to the super-sauze earthflow (Alpes-de-Haute-Provence, France). Geomorphology 43(2002):33–54

Malet J-P, van Asch TWJ, van Beek LPH, Maquaire O (2005) Forecasting the behavior of complex landslides with a 2-5D spatially distributed hydrological model. Nat Hazards Earth Syst Sci 5:1–15

Maugeri M, Motta E, Raciti E (2006) Mathematical modeling of the landslides occurred at Gagliano Castelferrato (Italy). Nat Hazards Earth Syst Sci 6:133–143

Mayoraz F, Vulliet L (2002) Neural networks for slope movement prediction. Int J Geomech 2(2):153–173

Mayoraz F, Cornu T, Vulliet L (1996) Using neural networks to predict slope movements. In: Senneset K (ed) Proc. 7th Int. Symp. on Landslides, Trondheim, Norway. Balkema, Rotterdam, pp 295–300

Michiue M (1985) A method for predicting slope failures on cliff and mountain due to heavy rain. J Nat Disaster Sci 7(1):1–12

Mufundirwa A, Fujii Y, Kodama J (2010) A new practical method for prediction of geomechanical failure-time. Int J Rock Mech Min Sci 47(7):1079–1090

Petley DN, Bulmer MH, Murphy W (2002) Patterns of movement in rotational and translational landslides. Geology 30(8):719–722

Petley DN, Mantovani F, Bulmer MH, Zannoni A (2005) The use of surface monitoring data for the interpretation of landslide movement patterns. Geomorphology 66:133–147

Pinault J–L, Schomburgk S (2006) Inverse modeling for characterizing surface water/groundwater exchanges. Water Resour Res 42:W08414. doi:10.1029/2005WR004587

Pouya A, Léonard C, Alfonsi P (2007) Modelling a viscous rock joint activated by rainfall: application to the La Clapière landslide. Int J Rock Mech Min Sci 44:120–129

Rose ND, Hungr O (2007) Forecasting potential rock slope failure in open pit mines using the inverse velocity method. Int J Rock Mech Min Sci 44(2):308–320

Sirangelo B, Versace P (1992) Modelli stocastici di precipitazione e soglie pluviometriche di innesco dei movimenti franosi. Florence, Italy, pp D361–D373

Sirangelo B, Versace P, Capparelli G (2003) Forewarning model for landslides triggered by rainfall based on the analysis of historical data file. Proceedings of the International Symposium "Hydrology of the Mediterranean and Semiarid Regions", vol 278. IAHS Publ, Montpellier, pp 289–304

Spickermann A, van Asch TWJ, Malet J-P (2009) Failure models and mechanisms in cohesive slopes; theoretical and numerical analysis of field and laboratory triggered events. In: Picarelli L, Tommasi P, Urcioli G, Versace P (eds) Proceedings of the IWL: rainfall induced landslides, vol 1. CIRIAM, Napoli, pp 103–110

Travelletti J, Malet J-P (2012) Characterization of the 3D geometry of flow-like landslides: a methodology based on the integration of heterogeneous multi-source data. Eng Geol 128:30–48

van Asch TWJ, Malet J-P (2009) Flow-type failures in fine-grained soils: an important aspect in landslide hazard analysis. Nat Hazards Earth Syst Sci 9:1703–1711

van Asch TWJ, Malet J-P, van Beek LPH (2006) Influence of landslide geometry and kinematic deformation to describe the liquefaction of landslides: Some theoretical considerations. Eng Geol 88(1–2):59–69

van Asch TWJ, Malet J-P, van Beek LPH, Amitrano D (2007a) Techniques, advances, problems and issues in the modelling of landslide hazard. Bull Soc Geol Fr 178(2):6–35

van Asch TWJ, van Beek LPH, Bogaard TA (2007b) Problems in predicting the mobility of slow-moving landslides. Eng Geol 91:46–55

Versace P, Capparelli G (2008) Empirical hydrological models for early warning of landslides induced by rainfall, Proceedings 1st World Landslide Forum, Tokyo, 18–21 November 2008, 627–630

Voight B (1988) A method for prediction of volcanic eruptions. Nature 332:125–130

Wieczorek GF (1987) Effect of rainfall intensity and duration on debris flows in central Santa Cruz Mountains, California. Rev Eng Geol VII:93–104

Zvelebill J, Moser M (2001) Monitoring based time-prediction of rock falls: three case-histories. Phys Chem Earth 26(2):159–167

S. Bernardie (✉) · N. Desramaut · M. Gourlay · G. Grandjean
BRGM, Orléans, France
e-mail: s.bernardie@brgm.fr

J.-P. Malet
Institut de Physique du Globe de Strasbourg, CNRS UMR 7516, EOST,
Université de Strasbourg, Strasbourg, France